

## $\gamma$ -Alumina as a Support for Catalysts: A Review of Fundamental Aspects

Monica Trueba\*<sup>[a]</sup> and Stefano P. Trasatti<sup>[a]</sup>

**Keywords:** Alumina / Materials science / Micro- and macrostructures / Supported catalysts

The present review discusses the most important aspects to take into consideration to improve the properties of  $\gamma$ -Al<sub>2</sub>O<sub>3</sub> as a support for catalytic applications. We show that the synthetic route to  $\gamma$ -Al<sub>2</sub>O<sub>3</sub> is the starting point that determines the micro- and macrostructure of the oxide and, consequently, allows control of the support characteristics. The relevance of the adequate structural characterization of the oxide as well as of its surface sorption behavior through the

proton-affinity distributions, are considered. The usefulness of the latter during supported catalyst preparation, for catalytic active sites characterization, and for stability evaluation after calcination are discussed for the Co/ $\gamma$ -Al<sub>2</sub>O<sub>3</sub> system in particular.

(© Wiley-VCH Verlag GmbH & Co. KGaA, 69451 Weinheim, Germany, 2005)

### 0. Introduction

Among the different transition aluminas known,  $\gamma$ -alumina ( $\gamma$ -Al<sub>2</sub>O<sub>3</sub>) is perhaps the most important with direct application as a catalyst and catalyst support in the automotive and petroleum industries.<sup>[1,2]</sup> The usefulness of this oxide can be traced to a favorable combination of its textural properties, such as surface area, pore volume, and pore-size distribution and its acid/base characteristics, which are

mainly related to surface chemical composition, local microstructure, and phase composition. Nevertheless, the chemical and hydrothermal stability of  $\gamma$ -Al<sub>2</sub>O<sub>3</sub> are still a critical point for catalytic applications.

For example, the use of  $\gamma$ -Al<sub>2</sub>O<sub>3</sub> as a support for Co-based catalysts in the Fischer–Tropsch (FT) process for the production of clean fuels<sup>[3,4]</sup> is not lacking in practical problems. The most common undesirable situations are: 1) alumina dissolution during supported catalyst preparation (usually in aqueous media), which affects the nature of the resulting Co species, 2)  $\gamma$ -Al<sub>2</sub>O<sub>3</sub> rehydration during catalyst implementation because of the H<sub>2</sub>O produced in the FT process, and 3) thermal degradation (sintering and phase transformation) in the catalyst regeneration step (hot-

[a] Department of Physical Chemistry and Electrochemistry, University of Milan,  
Via C. Golgi 19, 20133, Milan, Italy  
Fax: +39-02-5031-4300  
E-mail: monica.trueba@unimi.it



*Monica Trueba is a Ph.D. student in the Department of Physical Chemistry and Electrochemistry at the University of Milan (Italy). She is working on alumina supports for catalytic applications.*



*Stefano P. Trasatti is presently a researcher in the Physical Chemistry and Electrochemistry Department of the University of Milan. He received a PhD in Industrial Chemistry in 1995. In the same year he was awarded the Oronzio De Nora prize for the best work in the field of electrochemistry. He worked in a private company from 1996 to 2002 where he was responsible for surface treatments and material testing. He is the author of more than 20 papers and two patents in the field of metallic corrosion. His research interests include corrosion in refinery, corrosion monitoring and control, as well as the use of artificial intelligence systems in the study of corrosion.*

**MICROREVIEWS:** This feature introduces the readers to the authors' research through a concise overview of the selected topic. Reference to important work from others in the field is included.

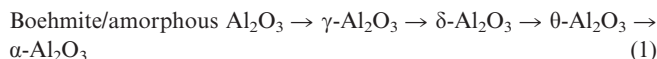
spots). It is clear that these side-reactions, which affect catalyst stability, activity, and selectivity, are principally related to support stability.

In the present work, the main aspects to be taken into account when trying to improve the properties of  $\gamma$ - $\text{Al}_2\text{O}_3$  as a support for catalysts are reviewed. First, the micro- and macroscopic nature of the support are described because without an adequate knowledge of them any applications will always be less than optimal. Next, the significance of the synthesis route is discussed, followed by the  $\gamma$ - $\text{Al}_2\text{O}_3$ /H<sub>2</sub>O interface and acid/base properties due to the effect of H<sub>2</sub>O on support stability during both catalyst preparation and implementation. The importance of studying the oxide surface sorption behavior through the proton-affinity distributions is also considered. Finally, some practical implications for the Co/ $\gamma$ - $\text{Al}_2\text{O}_3$  system are presented.

## 1. $\gamma$ -Alumina Structure

### 1.1. Microstructure

The principal features of the  $\gamma$ - $\text{Al}_2\text{O}_3$  microstructure are usually reported for the oxide obtained by the thermal dehydration (calcination) of aluminum hydroxides and oxyhydroxides. The transformation sequence during this process has been studied for many years, and it also gives other metastable phases of  $\alpha$ - $\text{Al}_2\text{O}_3$  depending on the calcination temperature [Equation (1)].<sup>[2,5–10]</sup>



$\gamma$ - $\text{Al}_2\text{O}_3$  is reported to appear at temperatures between 350 and 1000 °C when it is formed from crystalline<sup>[11]</sup> or amorphous<sup>[12]</sup> precursors, and is stable at temperatures as high as 1200 °C when the latter is used as the starting material.

The structural characterization of  $\gamma$ - $\text{Al}_2\text{O}_3$  is commonly performed by techniques such as IR spectroscopy,<sup>[6,13–16]</sup> NMR spectroscopy,<sup>[10,14,15,17]</sup> X-ray diffraction (XRD),<sup>[10,14,17,18]</sup> transmission electron microscopy (TEM),<sup>[16,19]</sup> and BET adsorption.<sup>[16,17]</sup> Additional information from the use of relatively new methods such as neutron vibrational spectroscopy (NVS), prompt-gamma activation analysis (PGAA), and small-angle X-ray scattering (SAXS), is also available.<sup>[10,16]</sup> Nevertheless, despite the variety of experimental and computational<sup>[9,20,21]</sup> studies, there is still a considerable debate about the structure of  $\gamma$ - $\text{Al}_2\text{O}_3$  as well as many of the transitional  $\text{Al}_2\text{O}_3$  phases.

The structure of  $\gamma$ - $\text{Al}_2\text{O}_3$  is traditionally considered as a cubic defect spinel type, whose experimental unit cell is illustrated in Figure 1. The defective nature derives from the presence of only trivalent Al cations in the spinel-like structure, i.e., the magnesium atoms in the ideal spinel  $\text{MgAl}_2\text{O}_4$  are replaced by aluminum atoms. The oxygen lattice is built up by a cubic close-packed stacking of oxygen layers, with Al atoms occupying the octahedral and tetrahedral sites. To satisfy the  $\gamma$ - $\text{Al}_2\text{O}_3$  stoichiometry some of the

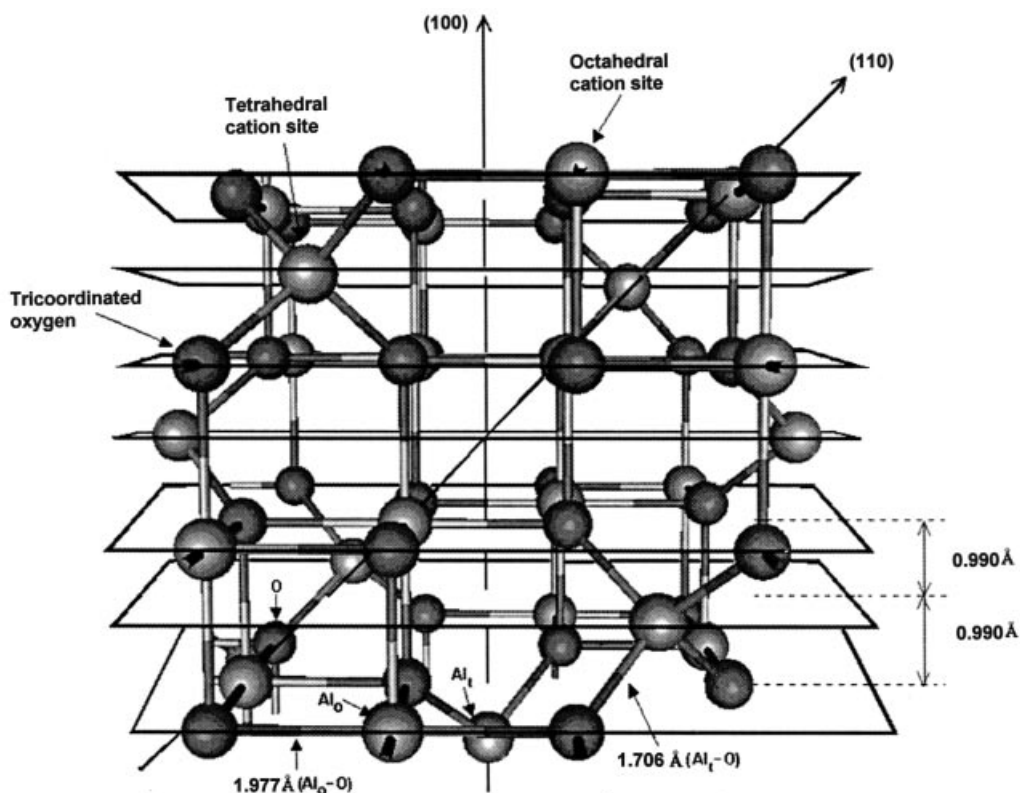


Figure 1. Experimental cubic  $\gamma$ - $\text{Al}_2\text{O}_3$  spinel-type unit cell.<sup>[21]</sup>

lattice positions remain empty (vacancies), although their precise location is still controversial.

When  $\gamma$ - $\text{Al}_2\text{O}_3$  is derived from amorphous aluminas it has always been reported to possess a cubic lattice.<sup>[12,22–25]</sup> Both a cubic lattice<sup>[26–28]</sup> and tetragonal distortion<sup>[29,30]</sup> are found for boehmite  $[\text{AlO}(\text{OH})]$ - or gibbsite  $[\text{Al}(\text{OH})_3]$ -derived  $\gamma$ - $\text{Al}_2\text{O}_3$ . Other studies, however, have proposed the existence of only a tetragonal structure.<sup>[10,16,31]</sup> Recently, tetragonal  $\gamma$ - $\text{Al}_2\text{O}_3$  obtained from highly crystalline boehmite was reported to be present between 450–750 °C.<sup>[10]</sup> A reduction of the tetragonal distortion can be produced by increasing the temperature, but at no stage is cubic  $\gamma$ - $\text{Al}_2\text{O}_3$  obtained. A new phase has been identified with more obvious cation ordering above 750 °C, designated as  $\gamma'$ - $\text{Al}_2\text{O}_3$ , which approaches the structure of  $\delta$ - $\text{Al}_2\text{O}_3$  above 900 °C.

It should be pointed out that some discrepancies exist with respect to the  $\delta$ -phase, which is usually an intermediate phase between  $\gamma$ - and  $\theta$ - $\text{Al}_2\text{O}_3$  [Equation (1)]. Some studies have reported that there is no distinct difference between  $\delta$ - and  $\gamma$ - $\text{Al}_2\text{O}_3$ .<sup>[30,32]</sup> The main difference is considered to be in the arrangement of the Al atoms: the vacancies are distributed between octahedral and tetrahedral sites in  $\gamma$ - $\text{Al}_2\text{O}_3$ , while they are only in octahedral sites in  $\delta$ - $\text{Al}_2\text{O}_3$ ; the oxygen lattice is the same for both phases. Other works, however, report no occurrence of the  $\delta$ -phase at all.<sup>[7,11]</sup>

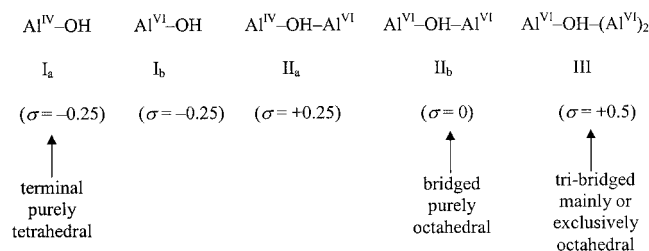
Many studies of  $\gamma$ - $\text{Al}_2\text{O}_3$  by means of XRD, NMR spectroscopy, and TEM have demonstrated the preference for vacancies in octahedral sites with the Al cation in tetrahedral positions,<sup>[7,26,28]</sup> whereas other authors support the opposite conclusion, i.e., the vacancies tend to reside in tetrahedral positions.<sup>[15,29]</sup> On the other hand, it has also been suggested that the cationic vacancies should be more realistically imagined as being distributed randomly between tetrahedral and octahedral cavities.<sup>[30]</sup> Further, it has also been reported that  $\gamma$ - $\text{Al}_2\text{O}_3$  contains significant portions of cations occupying “non-spinel” sites, i.e., sites that are vacant in the ideal spinel structure.<sup>[27]</sup>

The role of hydrogen has also been stressed. Some works claim that a considerable amount of hydrogen is present in the bulk structure of  $\gamma$ - $\text{Al}_2\text{O}_3$ ,<sup>[7,13,33,34]</sup> although the possibility of the hydrogen spinel ( $\text{HAl}_5\text{O}_8$ ) as a structural candidate instead of the OH species has been ruled out.<sup>[14,27,34]</sup> Computational studies show that this spinel structure is thermodynamically unstable.<sup>[9]</sup> A relatively well-ordered bulk crystalline  $\gamma$ - $\text{Al}_2\text{O}_3$  that contains no interstitial hydrogen has been reported in recent studies<sup>[16]</sup> where the H-containing species are localized at the surface and within amorphous regions.

The removal of OH groups during high temperature treatment creates coordinatively unsaturated surface (*cus*) cations where tetrahedral ( $\text{Al}^{\text{IV}}$ ) and octahedral ( $\text{Al}^{\text{VI}}$ ) aluminum coordinations are the most widely accepted.<sup>[10,14,35]</sup> However, variable amounts of pentahedrally coordinated aluminum ( $\text{Al}^{\text{V}}$ ), concentrated principally at the surface, have also been found.<sup>[13,15,36,37]</sup> It has been reported that the  $\text{Al}^{\text{V}}$  content is strictly related to the pore-size distribution, crystallinity, and surface area such that a high  $\text{Al}^{\text{V}}$  amount implies low crystallinity and a high surface area.<sup>[13]</sup> Three-

coordinate Al on the surface is unlikely, despite the fact that its presence would be expected based on the bulk structure.<sup>[14]</sup> The partly uncoordinated metal cations and oxide anions that lie at the surface of  $\gamma$ - $\text{Al}_2\text{O}_3$  can act as acids and bases, respectively, according to the Lewis definition.<sup>[35]</sup> The strongest acid sites are considered to be the  $\text{Al}^{\text{IV}}_{\text{cus}}$  ions, which are mainly located in crystallographically defective configurations and are responsible for the high catalytic activity of highly dehydrated aluminas. Nevertheless, the defective configurations, which yield the reactive surface sites, tend to be annihilated during high-temperature dehydration. The tendency of the Al coordination number to be lowered on  $\text{H}_2\text{O}$  desorption produces a new kind of OH group. The last OH groups to be removed are not related to those which were present on the initial hydroxylated surface and whose structure determines the properties of the *cus* surface cations.

The most important surface features of  $\gamma$ - $\text{Al}_2\text{O}_3$  have been determined by means of IR<sup>[6,35,38]</sup> and NMR spectroscopy,<sup>[38–40]</sup> although the precise nature of the surface acid sites is still unknown. Up to now, the most accepted and frequently used empirical model to describe  $\gamma$ - $\text{Al}_2\text{O}_3$  surfaces was that developed by Knözinger and Ratnasamy.<sup>[6]</sup>



Accordingly, five different types of OH groups are present on the surface that exhibit a distinct “net electric charge” ( $\sigma$ ), depending on the number of Al neighbors and on Al coordination. This model, however, has serious limitations due to its crude description of ideal  $\gamma$ -alumina surfaces that neglects surface hydroxylation/dehydroxylation process induced by temperature effects. Recently, using density functional (DFT) calculations, realistic models of the  $\gamma$ - $\text{Al}_2\text{O}_3$  surface have been proposed that account for the above process.<sup>[41]</sup> These models show that the behavior of various types of surface hydroxy groups depends strongly on the local chemical environment, morphology (exposed surfaces), and composition of the oxide, which are greatly influenced by the alumina precursors (starting materials) and synthetic methods used.

## 1.2. Macrostructure

Conventional  $\gamma$ -alumina is typically prepared by thermal dehydration of coarse particles of well-defined boehmite at a temperature above 400–450 °C.<sup>[2]</sup> The oxide obtained usually presents a surface area and pore volume below

Table 1. Point of zero charge (*pzc*) of  $\gamma$ -Al<sub>2</sub>O<sub>3</sub>.

Preparation procedure	Experimental method	<i>pzc</i>
Thermal treatment and aging of the hydrolysis product of Al ethoxide Commercial (Degussa Corp.)	Microelectrophoresis <sup>[69]</sup>	6.7–9.2
	Direct potentiometric titration <sup>[73]</sup>	8.6
	back titration <sup>[73]</sup>	7.5
	Mass titration <sup>[79]</sup>	8.3
Commercial (American Cyanamid)	Direct potentiometric titration <sup>[77]</sup>	7.0
Commercial (American Cyanamid)	$\gamma$ -Al <sub>2</sub> O <sub>3</sub> modified with F <sup>−</sup>	3.4
	at different temperatures <sup>[80]</sup>	6.3–8.0
	Potentiometric titration and electrophoresis <sup>[81]</sup>	8.0
	Discontinuous titration <sup>[74]</sup>	6.7
Commercial (Alfa Aesar)	Direct potentiometric titration <sup>[49]</sup>	8.25
Commercial (Condea)	$\gamma$ -Al <sub>2</sub> O <sub>3</sub> (5–10% $\delta$ -phase)	not <i>cip</i>
	$\gamma$ -Al <sub>2</sub> O <sub>3</sub> (56% $\delta$ -phase)	5.7
	$\gamma$ -Al <sub>2</sub> O <sub>3</sub> + 5% silica	6.9
	$\gamma$ -Al <sub>2</sub> O <sub>3</sub> + 5% zirconium	7.5
	$\gamma$ -Al <sub>2</sub> O <sub>3</sub> + 5% lanthanum	

250 m<sup>2</sup> g<sup>−1</sup> and 0.50 cm<sup>3</sup> g<sup>−1</sup>, respectively. Also, its stability is greatly affected by steam, which accelerates the transformation of  $\gamma$ -Al<sub>2</sub>O<sub>3</sub> into  $\alpha$ -Al<sub>2</sub>O<sub>3</sub>, with a consequent marked drop of surface area as a result of sintering.

Besides thermal decomposition, several methods for  $\gamma$ -Al<sub>2</sub>O<sub>3</sub> synthesis that use traditional techniques of preparative chemistry, such as precipitation and hydrolysis, have been developed to improve the oxide's textural properties and hydrothermal stability.<sup>[17,19,33,42–47]</sup> Moreover, the addition of thermal stabilizing modifiers (Zr<sup>4+</sup>, Ca<sup>2+</sup>, Th<sup>4+</sup>, and La<sup>3+</sup>) is quite popular. The latter inhibit the transformation of transition aluminas into the  $\alpha$ -phase, opposite to the effect obtained with In<sup>3+</sup>, Ga<sup>3+</sup>, and Mg<sup>2+</sup>. However, the acid-base behavior of the modified oxide can be very different with respect to the  $\gamma$ -Al<sub>2</sub>O<sub>3</sub> itself (Table 1).<sup>[48,49]</sup> The Al<sub>2</sub>O<sub>3</sub>-SiO<sub>2</sub> system has also been widely studied.<sup>[50–53]</sup>

Since the transition of metastable phases into  $\alpha$ -Al<sub>2</sub>O<sub>3</sub> occurs predominantly at the contact between primary particles, the key for suppressing the rate of sintering (without additives) is to prepare active aluminas in a morphological state in which the area of contact between primary particles is minimized, such as those with a fibrillar crystalline structure.<sup>[33]</sup> It is well known that microcrystalline solids show slower decomposition kinetics (e.g. dissolution).<sup>[54]</sup> Furthermore, it is preferable to avoid high-temperature treatments during calcination/decomposition of hydroxide and/or oxide mixtures because the solid-state reactions could be affected.

The past few years have witnessed marked progress in the synthesis of  $\gamma$ -aluminas. Due to the recent advancements in mesostructured silicas and other oxides,<sup>[55,56]</sup> efforts have been devoted to the synthesis of mesostructured aluminas with a well-ordered arrangement of pores that is essentially preserved after calcination. Many attempts have been made to synthesize ordered mesoporous alumina by supramolecular templating methods, where nonionic, anionic or cationic surfactants, or nonsurfactant molecules have been used as structural directing agents for the synthesis.<sup>[17,57–61]</sup> However, most of the aluminas obtained in this way present

mainly amorphous framework walls that limit their hydrothermal stability, which greatly compromises their usefulness in catalytic applications.

A novel three-step assembly pathway for the formation of a mesostructured alumina with framework pore-walls made of crystalline, lathlike  $\gamma$ -Al<sub>2</sub>O<sub>3</sub> nanoparticles has been reported recently.<sup>[62–64]</sup> The textural properties, like surface area and pore volume (300–350 m<sup>2</sup> g<sup>−1</sup> and 0.45–0.75 cm<sup>3</sup> g<sup>−1</sup>, respectively), are improved with respect to the conventional  $\gamma$ -alumina. Moreover, the morphological characteristics obtained, i.e., crystallinity and fibrillar-like structure, greatly improve the oxide's thermal and hydrolytic stability. These new mesostructures can be readily impregnated with transition metal precursors from aqueous solutions without loss of porosity, surface area, or pore volume, thus making them promising for applications in catalysis.

Sol-gel is the preferred method for the synthesis of aluminosilicates since it provides a low-temperature synthesis with excellent control over mixing.<sup>[50]</sup> In particular, slow simultaneous hydrolysis of the two alkoxides (precursors) is preferred to pre-hydrolysis since a higher yield of heterolinkages can be obtained. It has been shown that the nature of the precursor and the manner in which precursor hydrolysis is performed determine the properties of the resulting Al<sub>2</sub>O<sub>3</sub>-SiO<sub>2</sub> mixed oxide.<sup>[52,53]</sup> A decrease of the surface area (larger than the single oxides) with an increase of silica amount is obtained when aluminosilicates are prepared by slow simultaneous hydrolysis of Al and Si precursors.<sup>[53]</sup> A different tendency is reported for alumina-silica xerogels obtained by pre-hydrolysis.<sup>[52]</sup>

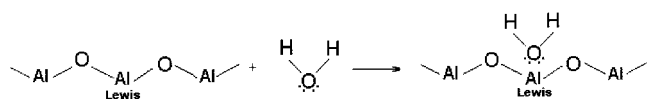
The wide experimental evidence indicates that the preparation history has an important effect on the type of  $\gamma$ -Al<sub>2</sub>O<sub>3</sub> structure that is produced (phase composition, bulk and surface chemical composition, and local microstructure of the oxide) as well as on oxide stability and textural properties. The reaction sequence and kinetics depend on the properties of the precursor and this applies not only to its different forms, for example gelatinous or highly crystalline



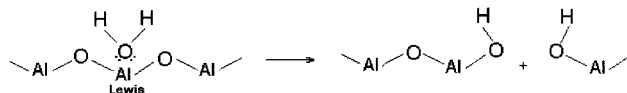
types, but also to the conditions under which the precursor is prepared.

## 2. $\gamma$ - $\text{Al}_2\text{O}_3/\text{H}_2\text{O}$ Interface

The existence of Lewis acid sites (*cus* cations) and basic sites (oxide anions) at the  $\gamma$ - $\text{Al}_2\text{O}_3$  surface allows its rehydroxylation (or rehydration) by interaction with  $\text{H}_2\text{O}$ , so that *cus* cations and anions can, in part, be converted into surface hydroxy groups.<sup>[6,13,21,35,37]</sup> This interaction has been represented as a two-step process for  $\gamma$ - $\text{Al}_2\text{O}_3$  under atmospheric conditions<sup>[21,37]</sup> that involves nondissociative adsorption of  $\text{H}_2\text{O}$  on Lewis sites (*cus* Al), which essentially consists in a transfer of electron density to a Lewis acid site



followed by dissociative chemisorption of  $\text{H}_2\text{O}$  and modification of surface Al coordination with the hydroxy group bonded to the Al atom, i.e., the two-coordinate oxygen atom adjacent to the Al site is protonated.



The rehydration of  $\gamma$ -alumina corresponds to the loss of tetrahedrally coordinated Al surface species and an increase of hydroxylated octahedral Al that can also involve some  $\text{Al}^{\text{IV}}$ .<sup>[13]</sup> The reactivity towards water depends on the layers exposed at each surface.

When the oxide particles are dispersed in water, the surface oxo and hydroxo groups at the solid/solution interface can associate with protons to form positively charged surface complexes.<sup>[33,54,65]</sup> The term “surface complex” does not imply a particular bonding structure but is used simply to indicate that chemical and/or noncoulombic physical interactions between the ionized surface sites and the associating ion lead to a kind of surface complex. The proton binding by oxo or hydroxy groups produces  $-\text{OH}$  and  $-\text{OH}_2$  species at the surface that will react according to their own proton affinity constant [Equations (2) and (3)].<sup>[33]</sup>



where  $K_i^{\Sigma v-2}$  and  $K_i^{\Sigma v-1}$  represent the intrinsic affinity constants that depend, for various types of surface groups, on the local configuration of the surface, especially the number ( $n$ ) of surrounding metal (M) cations and their effective bond valence ( $v$ ). It follows that the oxide/solution interface may be very complex and consist of different surface species that can reside at the same time on the oxide surface.

As a result of  $\gamma$ - $\text{Al}_2\text{O}_3$  surface/ $\text{H}_2\text{O}$  interactions, the dissolution of the alumina oxide may be induced by adsorption of  $\text{H}^+$  ions.<sup>[54,65]</sup> Earlier, the extent of dissolution was assumed to be controlled by thermodynamics. Presently, there is general agreement that this process is often controlled by slow chemical reactions occurring at the oxide/ $\text{H}_2\text{O}$  interface.<sup>[66–68]</sup> A dissolution reaction, more akin to etching, takes place preferentially along crystal defects induced by dislocations that may considerably accelerate kinetic processes while exerting only slight effects on the thermodynamic properties. The OH groups of the alumina surface determine not only its chemical and electrochemical properties but also the activity in the etching process. Thus, release of Al ions can be affected by any process that modifies the hydroxy group coverage of the oxide, such as temperature of calcination and cooling conditions, adsorption on surfaces, irreversible exchange of OH groups, etc.

Studies dedicated to clarifying the dissolution mechanism of anodic polycrystalline alumina membranes<sup>[67]</sup> have shown that the ratio of Al ion release into the solution depends on the alumina preparation, electrolyte conditions, such as ionic strength, and surface rehydroxylation. The authors considered that the different types of Al ions present on the surface are more active during the first treatment, since a decrease of the concentration of Al ions in solution is obtained upon repeated treatment with acid or base. They suggested that continuation of the etching is preceded by the rehydroxylation or hydrolysis of Al–O–Al bonds [Equation (4)]:



It is worth mentioning that the adsorption of small amounts of alumina on the surface of amorphous silica reduces the rate of silica dissolution in water even when much less than a monolayer of aluminum ions is present.<sup>[51]</sup> It has been postulated that negative aluminosilicate ion sites on the surface prevent hydroxy ions, which are required to catalyze the dissolution of silica, from approaching the interface.

## 3. Acid/Base Properties of $\gamma$ - $\text{Al}_2\text{O}_3$

### 3.1. General Considerations

Most solid oxides develop pH-dependent surface charges when immersed in aqueous solution, according to the general equilibria given in Equations (5) and (6).<sup>[33,65,68,70]</sup>



where  $\equiv\text{S}_{\text{basic}}\text{–OH}$  and  $\equiv\text{S}_{\text{acid}}\text{–OH}$  represent hydrated sites at the oxide surface with basic and acidic character and may have different local configurations. Depending on the concentration of either one or another type of sites, the oxides may show a dominant tendency to adsorb cations ( $\text{SiO}_2$ ,  $\text{SiO}_2\text{–Al}_2\text{O}_3$ , zeolites), anions ( $\text{MgO}$ ,  $\text{La}_2\text{O}_3$ ,  $\text{ZnO}$ ), or

both cations in basic solution and anions in acidic solution ( $\text{Al}_2\text{O}_3$ ,  $\text{TiO}_2$ ,  $\text{Cr}_2\text{O}_3$ ).

Acid and basic sites behave exactly as acid and basic substances in solution. Therefore, they respond reversibly to a change in solution pH with the concomitant variation of the total surface charge, with the  $\text{H}^+$  and  $\text{OH}^-$  ions usually being regarded as potential determining ions (absence of specific adsorption).

If  $\Gamma_{\text{OH}^-}$  is the surface concentration of negatively charged groups and  $\Gamma_{\text{H}^+}$  is the surface concentration of positively charged groups, the net surface charge of the oxide ( $\sigma_{\text{ox}}$ ) is defined according to Equation (7),<sup>[71,72]</sup> where  $\Gamma$  is measured in  $\text{mol cm}^{-2}$  and  $\sigma_{\text{ox}}$  in  $\text{C cm}^{-2}$ .

$$\sigma_{\text{ox}} = F(\Gamma_{\text{H}^+} - \Gamma_{\text{OH}^-}) \quad (7)$$

The pH at which  $\sigma_{\text{ox}} = 0$ , that is where  $\Gamma_{\text{H}^+} = \Gamma_{\text{OH}^-}$ , is called the point of zero charge (*pzc*). This does not correspond to the situation of undissociated OH groups but more realistically to the condition of positive surface groups being at the same concentration as negative surface groups. Generally, the surface charge of solid oxide is positive at low pH and negative at high pH.

It should be pointed out that the terminology employed in the literature for “zero point” is plenty, and terms like isoelectric point of the solid (*ieps*),<sup>[69,70]</sup> point of zero salt effect (*pzse*),<sup>[73]</sup> point of zero net charge (*pznc*),<sup>[74]</sup> point of zero net proton charge (*pznpc*),<sup>[74–76]</sup> and pristine point of zero charge (*ppzc*)<sup>[77,78]</sup> can be found.

Besides *pzc*, another important quantity that characterizes oxide/solution interfaces is the isoelectric point (*iep*), which corresponds to the pH at which the so-called zeta ( $\zeta$ ) potential is zero.<sup>[70–72]</sup> This potential is related only to the presence of the free charges in the diffuse layer in solution and can be determined by means of electrokinetic experiments like electrophoresis.

According to the *pzc* and *iep* concepts, the difference between these characteristics is a substantial one. The *pzc* measures the condition of neutrality of the oxide surface while the *iep* is a measure of the condition of zero diffuse charge on the solution side. In the absence of specific adsorption the condition of neutrality corresponds to  $\sigma_{\text{ox}} = 0$  on the solution side, hence *pzc* = *iep*. If specific adsorption is present, the net charge in the liquid phase of the interface may be different from zero, i.e.,  $\zeta \neq 0$  and *pzc*  $\neq$  *iep*. Conversely, at the *iep*, the fact that the total charge is zero does not necessarily mean that  $\Gamma_{\text{H}^+} = \Gamma_{\text{OH}^-}$  due to the possible presence of extra charge associated with specifically adsorbed non-potential-determining ions.

The *pzc* is commonly determined by potentiometric titration<sup>[52,53,73,76,77,79–81]</sup> as these results can be directly converted into proton-adsorption isotherms. The relative surface concentration of protons is frequently obtained by mass balance between the proton (or hydroxide) ions added to solution and the measured proton concentration in solution at equilibrium.<sup>[53,73,77–80]</sup> The titration procedure is usually performed for different concentrations of the inert electrolyte, i.e., at different solution ionic strengths. If the potential-determining ions are  $\text{H}^+$  and  $\text{OH}^-$  for acid and

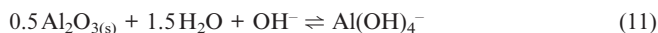
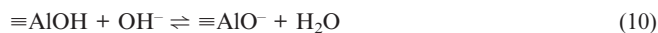
base titration, respectively (absence of specific adsorption), the titration (charging) curves as well as adsorption isotherms should pass through a common intersection point (*cip*), identified as *pzc*. It should be pointed out that potentiometric titration is reliable only if the amount of protons exchanged by the oxide sample is larger than that involved in the autoprotolysis of water, which is pH dependent.<sup>[82]</sup> Accordingly, the pH window whereby useful information is obtained is from pH = 3 to 11 (outside this region the buffering effect of  $\text{H}_2\text{O}$  prevails).

### 3.2. Point of Zero Charge of $\gamma\text{-Al}_2\text{O}_3$

The surface sorption behavior of  $\gamma\text{-Al}_2\text{O}_3$  has been widely studied, although the *pzc* for this oxide is not reported as a unique value or in a narrow range of pH values but between 6 and 9.<sup>[49,65,69,73,74,76,77,80–83]</sup> This is related mainly to the differences in material preparation that influence the micro- and macrostructure of the oxide, and to the experimental method used for *pzc* determination. General trends have been proposed, like the variation of the *pzc* with degree of sample hydration, impurities, structure defects, etc. Some of the available data are summarized in Table 1.

Recently, a discontinuous titration procedure that allows simultaneous measurement of protons and background electrolyte has shown that whereas proton adsorption/desorption gives rise to a positive/negative surface charge, Al dissolution does not.<sup>[74]</sup> This result supports previous studies which concluded that Al dissolution consumes  $\text{H}^+$  ions without affecting the surface charge.<sup>[73,84,85]</sup> For example, increasing the amounts of soluble Al or  $\text{CO}_2$  in solution lowers the phenolphthalein end-point (8.3) to 7.9 and 7–7.3, respectively.<sup>[85]</sup>

Two mechanisms of acid-base consumption have been proposed,<sup>[74]</sup> namely significant proton consumption at low values of pH as a result of either proton adsorption [Equation (8)] or Al dissolution [Equation (9)], and base consumption that reflects proton dissociation at higher pH (>6) [Equation (10)] and/or mineral dissolution [Equation (11)].



These two mechanisms cannot be distinguished on the basis of titration data alone, and independent measurement of the background ion adsorption and Al dissolution are required, as was stressed in other research papers.<sup>[76]</sup>

Traditional titration methods do not properly consider the solubility of  $\gamma\text{-Al}_2\text{O}_3$ , which is pH dependent, since various concentrations of Al in solution exert different effects on the shape of the colloidal titration curve. For a correct estimation of the adsorbed proton concentration only,

Schulthess and Parks<sup>[73]</sup> have developed a back-titration technique that allows the consideration of all sources that consume hydrogen ions and properly adjusts the titration curve for the changes in solubility as the pH changes. This method more accurately reveals the adsorption behavior of  $H^+$  on the surface of  $\gamma\text{-Al}_2\text{O}_3$ . In fact, the obtained *pzc* values differ by more than one pH unit as forwards (8.60) and back (7.50) titration is performed.

Several studies have demonstrated that polyvalent cations in electrolyte solution compete successfully with protons for adsorption on the active sites of the alumina surface by means of a cation–proton exchange reaction.<sup>[54,69,74,75,79,86,87]</sup> It has been shown that this process constitutes an alternative method for the estimation of dissolution active sites, since it inhibits oxide dissolution (blocking effect).<sup>[53]</sup>

For  $\gamma\text{-Al}_2\text{O}_3$ , specific cationic adsorption is proposed because the *cip* is localized in the alkaline pH region and the  $H^+$  adsorption is different from zero.<sup>[49,73,79,86]</sup> The common intersection point (*cip*), however, cannot be considered as the *pzc*, according to the previous definition. The competitive adsorption has been interpreted as follows.<sup>[73]</sup> If electrolyte cations/anions are specifically adsorbed over  $H^+/OH^-$  ions, an increase in apparent proton desorption/adsorption is produced. Each  $H^+/OH^-$  ion removed from the surface by cation/anion exchange would neutralize a  $OH^-/H^+$  species in solution and this would not be readily distinguished from  $H^+$  ion removal by adsorption. At the *cip*, the amounts of  $H^+$  and  $OH^-$  displaced from the surface site are equal and no apparent change in pH is detected with changes in salt concentration (ionic strength). The fact that the *cip* is not coincident with the *pzc* indicates that the surface charge is not equivalent to the proton isotherms, and at high ionic strengths only apparent proton isotherms are obtained due to electrolyte cation/anion competition. The asymmetry (*cip* shift) of the charging curves also depends on the nature of the electrolyte ions and/or on the presence of differently reacting crystal planes.

The effect of the amount of  $\gamma\text{-Al}_2\text{O}_3$  in solution on its surface behavior has also been investigated. It has been reported that the *pzc* decreases with concentration from about 9.5 at 1.0 wt.-% to 8.6 at 10 wt.-%,<sup>[76]</sup> thus indicating that the proton surface data obtained for dilute suspensions do not directly reflect the surface charge characteristics of concentrated suspensions. In a previous work it was found that the amount of oxide present in suspension does not influence the amount of protons consumed/released upon dissolution of  $\gamma\text{-Al}_2\text{O}_3$ ; however, the concentration of the solid in solution was considerably lower (1–3 wt.-%).<sup>[77]</sup>

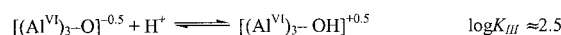
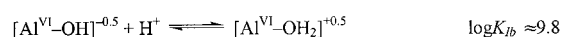
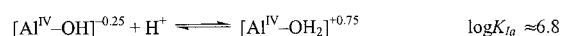
The acid-base properties of aluminosilicates have also been studied<sup>[33,50–53,88,89]</sup> due to the usefulness of these materials in catalytic applications. It has been reported that the surface charge and *pzc* of the mixed oxide increase with Al content,<sup>[53]</sup> although Lewis acid sites of similar strength are present on the surface independently of the Al/Si atomic ratio. Brønsted acidity also exists, especially in the samples with a higher percentage of silica, which arises from silanol groups (terminal silanol and bridging OH groups). The *pzc*

of  $\gamma\text{-Al}_2\text{O}_3\text{-SiO}_2$  also depends on the way  $\gamma\text{-Al}_2\text{O}_3$  silanization is performed as well as on the silanization agent. For example, the use of ethyltriethoxysilane instead of dimethyldimethoxysilane lowers the *pzc* value from 7.1 to 6.25.<sup>[49]</sup>

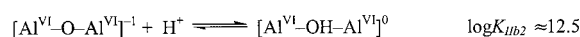
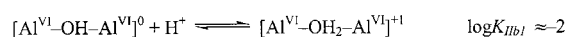
### 3.3. $\gamma\text{-Al}_2\text{O}_3$ Surface Heterogeneity

Heterogeneity effects in the adsorption of oxide/electrolyte solutions were first considered by Leckie et al. in 1978.<sup>[90]</sup> Since then, many models<sup>[65,78,81,87,91,92]</sup> as well as a great variety of materials such as inorganic metal oxides,<sup>[82,86,87,93]</sup> mixed oxides,<sup>[94]</sup> clays,<sup>[95–97]</sup> carbons,<sup>[98,99]</sup> and humic substances<sup>[100,101]</sup> have been used to describe proton-binding behavior at oxide/solution interfaces. Most site-binding models are a combination of surface reactions and an electrostatic approach, and these models can often describe proton adsorption data quite satisfactorily, although their physical chemistry picture is very different. As a result, an objective picture of the intrinsic properties of the oxide/solution interface is difficult to obtain due to the dependence of the calculated parameters on the specific model applied.

An important result derived from  $\gamma\text{-Al}_2\text{O}_3$  surface heterogeneity experimental studies<sup>[33,77,80]</sup> is the resolution of three or four categories of surface sites, making use of proton-binding isotherms from potentiometric titration and proton-affinity distributions. These sites contribute to proton binding and surface-charge development between pH = 3 and 11 and will react specifically with solution protons, depending on their  $\log K_i$  and solution pH, as follows:



Nonactive surface sites over the mentioned pH range have also been proposed:



Protonation of hydroxy groups is more difficult because of the proton–proton repulsion in the  $\text{-OH}_2$  species. Only surface hydroxy groups with negative uncompensated charge (types  $I_a$  and  $I_b$ , according to Knözinger and Ratnasamy<sup>[6]</sup>) can be protonated in the pH interval used.

A direct consequence of this is that at any pH the oxide surface exhibits sites which carry positive charges ( $\log K_i > \text{pH}$ ) and sites with negative charges ( $\log K_i < \text{pH}$ ), which are disposed in regular arrays on different crystal planes at the surface. Another consequence is that, even at the pH

corresponding to *pzc*, some of the above sites can still be charged.

A knowledge of the proton distribution and proton-binding properties for various surface sites (strength and number), synonymous of surface heterogeneity, is needed to predict the pH dependence of the surface charge. It has been shown that the occurrence of the *cip* in charging curves depends on the actual distribution of the surface sites.<sup>[49,73,77,93,102]</sup> This applies not only to  $\gamma$ - $\text{Al}_2\text{O}_3$  modified with anionic and/or cationic species but also when its phase composition changes. As illustrated in Table 1, no definite *cip* is obtained for  $\gamma$ - $\text{Al}_2\text{O}_3$  samples containing 56% of the  $\delta$ -phase<sup>[49]</sup> as a result of the increase of surface and bulk heterogeneity. Success in obtaining a meaningful and accurate proton adsorption distribution generally depends on the method of its evaluation, the quality of the experimental data, and the appropriate choice of adsorption model.<sup>[103]</sup> Among the variety of methods for the quantitative estimation of the surface heterogeneity of metal oxides,<sup>[103–106]</sup> a new method based on the determination of proton-affinity distribution by plotting titration data as derivatives of the proton/hydroxy ion adsorption as a function of pH has been proposed.<sup>[107]</sup> This approach is considered more realistic from a physical point of view.

Additional necessary information is the temperature dependence of the equilibrium constant and the influence of the temperature on the proton-affinity distribution at the oxide/electrolyte interface, both of which are also vital for any attempt at understanding proton-induced surface dissolution. Studies of the effect of temperature on the proton-affinity distribution at the  $\gamma$ - $\text{Al}_2\text{O}_3$ /electrolyte interface have shown that temperature variations can affect proton binding in a different way on various groups of surface sites, depending on their enthalpy and entropy changes for specific proton adsorption.<sup>[80]</sup> The effect of temperature and electrolyte is twofold: proton-affinity constants depend on temperature like all free-energy functions, but the development of the surface charge is also perturbed by electrostatic repulsion in the double layer, which is dependent on the electrolyte concentration.

It is worth mentioning that the use of proton-affinity distributions allows us to obtain reliable quantitative information on the Brønsted acidity of mixed oxide systems such as aluminosilicates.<sup>[33,52]</sup> Methods like IR<sup>[50]</sup> or titration with Hammett color indicators<sup>[108]</sup> often meet with the difficulty of separating the contributions of Brønsted and Lewis acidity.

The adsorption properties of oxides as a function of solution pH may be predicted, at least in principle, by the knowledge of their *pzc*. However, the heterogeneity of acid/base sites on their surface raises some questions about the significance of a global *pzc*. For every heterogeneous surface the concept of *pzc* must be more carefully considered, although, in reality, *pzc* is an overall surface property rather than a thermodynamically meaningful constant. The proton-binding properties for various surface sites allow us to predict the  $\gamma$ - $\text{Al}_2\text{O}_3$  adsorption capacity as a function of pH more accurately.

## 4. $\gamma$ - $\text{Al}_2\text{O}_3$ as a Support

### 4.1. General Aspects

Transition aluminas are frequently used as pre-shaped supports for preparing multiphase catalysts that consist of an active phase dispersed on a carrier or support.<sup>[33]</sup> The properties of the active phase depend mainly on the manner in which the active component of the catalyst (precursor) is introduced onto the support and the nature and strength of precursor–support interactions.

The major route for supported catalyst preparation makes use of aqueous media by simple impregnation (wet impregnation or incipient wetness) or by homogeneous deposition-precipitation, ion exchange, and specific adsorption. The choice of one or the other route is usually made by considering the nature and strength of the support–precursor interactions. Common subsequent steps are washing and drying, accompanied by irreversible transformation of the catalyst (its activation).

Different kinds of precursor–support interactions have been considered. Surface interactions for small ions are generally accepted to be predominantly electrostatic, which is supported by experimental results where the extent of adsorption of positive/negative ions increases with a pH rise/decrease. Nevertheless, some experimental evidence reflects exceptions from the simple rule of electrostatic adsorption with the existence of “specific” or “chemical” surface–adsorbate interactions that may compete with coulombic repulsion, as in the adsorption of cations such as  $\text{Ni}^{2+}$ ,  $\text{Co}^{2+}$ , and  $\text{Pb}^{2+}$  onto a positively charged alumina surface.<sup>[109,110]</sup> These results support the existence of specific sites on the hydroxylated surface that act in adsorption of the catalyst precursor and are related to the intrinsic acid/base properties of the surface. Moreover, the adsorption by ligand substitution, i.e., surface hydroxyls “become members” of the coordination sphere of the adsorbate, has been suggested for halide complexes of Pt, Pd, Rh, Ir, Au, and Ru on alumina<sup>[111]</sup> and for amine complexes of  $\text{Co}^{2+}$ ,  $\text{Ni}^{2+}$ , and  $\text{Cu}^{2+}$  on titania.<sup>[112]</sup>

The surface density of adsorption sites is usually low, which gives a high metal dispersion but insufficient loading. Regulation of the adsorption capacity of amphoteric supports like  $\gamma$ - $\text{Al}_2\text{O}_3$  can be done by doping solid oxides with electropositive ( $\text{Na}^+$ ,  $\text{Li}^+$ ) or electronegative ( $\text{F}^-$ ,  $\text{Cl}^-$ ) ions, which results in an increase/decrease of the apparent *pzc* values of supports. However, the introduction of basic or acidic modifiers may also change important properties of the catalysts (Table 1). Another possibility for increasing metal concentration is variation of the temperature of the impregnation solution.

In spite of the advantages of precursor impregnation from an aqueous phase, such as easy scale up at relatively low cost, the use of the metal is inefficient because of its incomplete loading and reduction and uncontrolled sintering during high-temperature salt decomposition. This has motivated researchers to study other ways to prepare supported catalysts, directed mainly at avoiding the use of  $\text{H}_2\text{O}$



as the impregnation phase.<sup>[33]</sup> Organic media, vapour, and solid phases have been investigated. The most straightforward way for preparing dispersed metal catalysts consists in mounting metallic atoms or small clusters of metal atoms in their zero-valent state onto an appropriate support, which eliminates the need for any subsequent activation and the catalyst can be obtained in a single preparation step. For example, metallic Pt particles mounted on TiO<sub>2</sub> by means of a microemulsion method have been reported recently.<sup>[47]</sup> Metal-support interactions are not observed and the Pt/TiO<sub>2</sub> catalysts show higher catalytic activity than the same material prepared by the impregnation technique.

## 4.2. Co/ $\gamma$ -Al<sub>2</sub>O<sub>3</sub> Catalysts

It is well known that supported catalysts containing metallic cobalt or as an oxide or sulfide are very important in heterogeneous catalysis. The actual interest is focused on the Co deposition mechanism and its dependence on the support surface features. It is not easy to explain why the maximum rate of deposition is obtained in the first stages of impregnation where a negligible amount of Al<sup>3+</sup> ions have been released, especially considering that  $\gamma$ -Al<sub>2</sub>O<sub>3</sub> surface dissolution is a slow process. A systematic kinetic study of Co<sup>2+</sup> deposition together with  $\gamma$ -Al<sub>2</sub>O<sub>3</sub> surface dissolution is thought to be the best way to clarify this mechanistic aspect.

Another important challenge is the elucidation of the local structure of the deposited Co<sup>2+</sup> species. The first direct evidence for the formation of inner sphere Co<sup>2+</sup> complexes on a  $\gamma$ -Al<sub>2</sub>O<sub>3</sub> surface was obtained in the 1990s by means of extended X-ray absorption fine-structure (EXAFS). At present, it is not clear why an Al-Co precipitate with a hydrotalcite structure predominates in the cases where the deposition of Co<sup>2+</sup> on  $\gamma$ -Al<sub>2</sub>O<sub>3</sub> takes place through the Co(H<sub>2</sub>O)<sub>6</sub><sup>2+</sup> species.

Studies to elucidate the mechanism of Co<sup>2+</sup> adsorption on  $\gamma$ -Al<sub>2</sub>O<sub>3</sub> have been developed since the early 1970s and were reviewed recently.<sup>[114]</sup> Most of the work reported uses Co<sup>II</sup> aqua complexes as precursors. In general, Co<sup>2+</sup> adsorption on  $\gamma$ -Al<sub>2</sub>O<sub>3</sub> increases considerably with solution pH in the range from 5 to 8, although the process becomes increasingly masked by precipitation of Co(OH)<sub>2</sub> at higher pH values. Restoring the initial pH value by addition of acid or base has been proposed since the decrease of impregnation solution pH during Co<sup>2+</sup> adsorption on  $\gamma$ -Al<sub>2</sub>O<sub>3</sub> decreases the extent of the deposition process markedly. In this way, Co<sup>2+</sup> precipitation inside the pores is avoided and Co/ $\gamma$ -Al<sub>2</sub>O<sub>3</sub> catalysts with very highly active surfaces can be obtained. The extent of adsorption can also be increased by increasing the temperature during impregnation, thus influencing the resulting structure of the adsorbate. For example, Co(OH)<sub>2</sub> predominates under ambient conditions while CoAl<sub>2</sub>O<sub>4</sub> becomes important at higher temperatures. Co<sup>2+</sup> adsorption has also been studied on  $\gamma$ -Al<sub>2</sub>O<sub>3</sub> modified with F<sup>-</sup> ions – the adsorption increases with higher F<sup>-</sup> content.

Studies of adsorption of Co<sup>2+</sup> and Ni<sup>2+</sup> amino complexes on  $\gamma$ -Al<sub>2</sub>O<sub>3</sub> have demonstrated that alumina should not be considered inert during impregnation, even under mild conditions such as at ambient temperature, with a pH close to the *pzc* of the support, and with reasonable contact times.<sup>[83,115]</sup> Alumina dissolution is promoted not only by protons or hydroxy ions but also by the presence of Co and Ni ions in solution. The authors suggest that the following phenomena take place at the same time at the  $\gamma$ -Al<sub>2</sub>O<sub>3</sub>/solution interface during impregnation:

- adsorption of ions which, in certain cases, may even accelerate the rate of support dissolution;
- dissolution of alumina, which depends on the characteristics of the alumina surface;
- precipitation of cations released from the support with metal ions in solution;
- alumina rehydration.

The use of proton-affinity distributions for characterization of the active sites of  $\gamma$ -Al<sub>2</sub>O<sub>3</sub>/Co and  $\gamma$ -Al<sub>2</sub>O<sub>3</sub>/Co-Mo catalysts has been reported.<sup>[113]</sup> Potentiometric titration in combination with proton-affinity distributions has been proposed as a powerful method for the characterization of a supported catalyst surface.

The picture that emerges from the recent literature emphasizes the importance of the intrinsic heterogeneity of adsorption sites on the support for catalyst preparation. The proton-binding properties of various surface sites, i.e. the pH-dependent surface development, are also needed when the precursor salt is present in solution. Another important issue is the stability of the Co<sup>2+</sup> complexes on  $\gamma$ -Al<sub>2</sub>O<sub>3</sub> and the evolution of the system during subsequent preparation steps such as drying and calcination for the evaluation of the properties of the supported catalyst (activity and selectivity).

## 5. Conclusions

There is no doubt that the preparation history of  $\gamma$ -Al<sub>2</sub>O<sub>3</sub> strongly determines its properties. Consequently, the phase composition, bulk and surface chemical composition, local microstructure, as well as stability and textural properties of the oxide can be controlled by varying the synthetic route for the application of  $\gamma$ -Al<sub>2</sub>O<sub>3</sub> as a catalyst support. The frequent use of aqueous media for supported catalyst preparation implies that rigorous  $\gamma$ -Al<sub>2</sub>O<sub>3</sub> characterization is important not only from a structural point of view. The oxide acid/base properties and adsorption capacity as a function of solution pH (and temperature) should be taken into consideration for both  $\gamma$ -Al<sub>2</sub>O<sub>3</sub>/electrolyte and  $\gamma$ -Al<sub>2</sub>O<sub>3</sub>/Co<sup>2+</sup> salt solution systems as only the *pzc* value is not enough. Information from surface heterogeneity can help to understand and to regulate the adsorption mechanism as well as the occurrence of secondary reactions such as  $\gamma$ -Al<sub>2</sub>O<sub>3</sub> dissolution. Further, the nature of the active sites of the supported catalyst and its stability should be evaluated prior to testing catalyst activity and selectivity.

- [1] K. Oberlander, *Applied Industrial Catalysis* (Ed.: B. E. Leach), Academic Press, New York, **1984**, p. 63.
- [2] K. Wefers, *Alumina Chemicals: Science and Technology Handbook* (Ed.: L. D. Hart), The American Ceramic Society, Westerville, Ohio, **1990**, p. 13.
- [3] M. E. Dry, *Appl. Catal. A: General* **1996**, *138*, 319–344.
- [4] C. L. Bianchi, *Catal. Lett.* **2001**, *76*, 155–159.
- [5] S. J. Wilson, M. H. Stacey, *J. Colloid Interface Sci.* **1981**, *82*, 507–517.
- [6] C. Morterra, G. Magnacca, *Catal. Today* **1996**, *27*, 497–532.
- [7] J. A. Wang, X. Bokhimi, A. Morales, O. Novaro, T. López, R. Gómez, *J. Phys. Chem. B* **1999**, *103*, 299–303.
- [8] K. Shimizu, Y. Kato, H. Yoshida, A. Satsuma, T. Hattori, T. Yoshida, *Chem. Commun.* **1999**, *17*, 1681–1682.
- [9] C. Wolverton, K. C. Hass, *Phys. Rev. B* **2000**, *63*, 1–16 024102-1–024102-16.
- [10] G. Paglia, C. E. Buckley, A. L. Rohl, R. D. Hart, K. Winter, A. J. Studer, B. A. Hunter, J. V. Hanna, *Chem. Mater.* **2004**, *16*, 220–236.
- [11] B. A. Latella, B. H. O'Connor, *J. Am. Ceram. Soc.* **1997**, *80*, 2941–2944.
- [12] T. C. Chou, D. Adamson, J. Mardinly, T. G. Nieh, *Thin Solid Films* **1991**, *205*, 131–139.
- [13] A. A. Tsyganenko, P. P. Mardilovich, *J. Chem. Soc., Faraday Trans.* **1996**, *92*, 4843–4852.
- [14] K. Sohlberg, S. J. Pennycook, S. T. Pantelides, *J. Am. Chem. Soc.* **1999**, *121*, 10999–11001.
- [15] C. Pecharroman, I. Sobrados, J. E. Iglesias, T. González-Carreño, J. Sanz, *J. Phys. Chem. B* **1999**, *103*, 6160–6170.
- [16] G. Paglia, C. E. Buckley, T. J. Udovic, A. L. Rohl, F. Jones, C. F. Maitland, J. Connolly, *Chem. Mater.* **2004**, *16*, 1914–1923.
- [17] V. González-Peña, I. Díaz, C. Márquez-Alvarez, E. Sastre, J. Pérez-Pariente, *Microporous Mesoporous Mater.* **2001**, *44–45*, 203–210.
- [18] A. K. Bhattacharya, D. R. Pyke, G. S. Walker, C. R. Werrett, *Appl. Surf. Sci.* **1997**, *108*, 465–470.
- [19] T. Ren, Z. Yuan, B. Su, *Langmuir* **2004**, *20*, 1531–1534.
- [20] X. Krokidis, P. Raybaud, A. Gobichon, B. Rebours, P. Euzen, H. Toulhoat, *J. Phys. Chem. B* **2001**, *105*, 5121–5130.
- [21] A. Ionescu, A. Allouche, J. P. Aycard, M. Rajzmann, F. Hutschka, *J. Phys. Chem. B* **2002**, *106*, 9359–9366.
- [22] I. Levin, L. A. Bendersky, D. G. Brandon, M. Ruhle, *Acta Mater.* **1997**, *45*, 3659–3669.
- [23] M. Plummer, *J. Appl. Chem.* **1958**, *8*, 35–44.
- [24] R. McPherson, *J. Mater. Sci.* **1973**, *8*, 851–858.
- [25] R. McPherson, *J. Mater. Sci.* **1980**, *15*, 3141–3149.
- [26] K. P. Sinha, A. P. B. Sinha, *J. Phys. Chem.* **1957**, *61*, 758–761.
- [27] R. S. Zhou, R. L. Snyder, *Acta Crystallogr., Sect. B* **1991**, *47*, 617–630.
- [28] Y. G. Wang, P. M. Bronsveld, J. Th. M. Dehosson, B. Djuricic, D. McGarry, S. Pickering, *J. Am. Ceram. Soc.* **1998**, *81*, 1655–1660.
- [29] S. J. Wilson, *J. Solid State Chem.* **1979**, *30*, 247–255.
- [30] S. J. Wilson, J. D. C. McConnell, *J. Solid State Chem.* **1980**, *34*, 315–322.
- [31] T. Tsuchida, R. Furuichi, T. Ishii, *Thermochim. Acta* **1980**, *39*, 103–115.
- [32] R. H. French, H. Mullejans, D. J. Jones, *J. Am. Ceram. Soc.* **1998**, *81*, 2549–2557.
- [33] J. A. Schwarz, C. Contescu, A. Contescu, *Chem. Rev.* **1995**, *95*, 477–510.
- [34] K. Sohlberg, S. J. Pennycook, S. T. Pantelides, *J. Am. Chem. Soc.* **1999**, *121*, 7493–7499.
- [35] G. Busca, *Catal. Today* **1998**, *41*, 191–206.
- [36] D. Coster, J. J. Fripiat, *Chem. Mater.* **1993**, *5*, 1204–1210.
- [37] D. Coster, J. J. Fripiat, M. Muscas, A. Auroux, *Langmuir* **1995**, *11*, 2615–2620.
- [38] K. Sohlberg, S. J. Pennycook, S. T. Pantelides, *Chem. Eng. Commun.* **2000**, *181*, 107–135.
- [39] C. S. John, N. C. M. Alma, G. R. Hays, *Appl. Catal.* **1983**, *6*, 341–346.
- [40] D. Coster, A. L. Blumenfeld, J. J. Fripiat, *J. Phys. Chem.* **1994**, *98*, 6201–6211.
- [41] M. Digne, P. Sautet, P. Raybaud, P. Euzen, H. Toulhoat, *J. Catal.* **2002**, *211*, 1–5.
- [42] S. F. Tikhov, V. B. Fenelonov, V. I. Zaikovskii, Yu. V. Potapova, V. A. Sadykov, *Microporous Mesoporous Mater.* **1999**, *33*, 137–142.
- [43] W. Deng, P. Bodart, M. Pruski, B. H. Shanks, *Microporous Mesoporous Mater.* **2002**, *52*, 169–177.
- [44] Nanotechnology in mesostructured materials: Y. Kim, Ch. Kim, J. W. Choi, P. Kim, J. Yi, *Stud. Surf. Sci. Catal.* **2003**, *146*, 209–212.
- [45] Ch. Kim, Y. Kim, P. Kim, J. Yi, *Korean J. Chem. Eng.* **2003**, *20*, 1142–1144.
- [46] M. I. F. Macedo, C. C. Osawa, C. A. Bertran, *J. Sol-Gel Sci. Technol.* **2004**, *30*, 135–140.
- [47] X. Zhang, F. Zhang, K. Chan, *Mater. Lett.* **2004**, *58*, 2872–2877.
- [48] Acidity and Basicity of Solids: A. Lycourghiotis, *ASI Series, Series C: Mathem. Phys. Sci.* **1994**, *444*, 415–444.
- [49] S. P. Trasatti, B. Sacchi, *Study of the Degradation Process of Catalyst Supports by Means of Electrochemical Techniques*, University of Milan, **2004**, Report 3/2004, p. 1–35.
- [50] J. B. Miller, E. I. Ko, *Catal. Today* **1997**, *35*, 269–292.
- [51] R. K. Iler, *J. Colloid Interface Sci.* **1973**, *43*, 399–408.
- [52] T. J. Bandosz, C. Lin, J. A. Ritter, *J. Colloid Interface Sci.* **1998**, *198*, 347–353.
- [53] V. La Parola, G. Deganello, S. Scirè, A. M. Venezia, *J. Solid State Chem.* **2003**, *174*, 482–488.
- [54] B. Wehrli, E. Wieland, G. Furrer, *Aquat. Sci.* **1990**, *52*, 1–31.
- [55] P. Yang, D. Zhao, D. I. Margolese, B. F. Chmelka, G. D. Stucky, *Nature* **1998**, *396*, 152–155.
- [56] A. Sayari, S. Hamoudi, Y. Yang, I. L. Moudrakovski, J. R. Ripmeester, *Chem. Mater.* **2000**, *12*, 3857–3863.
- [57] S. Cabrera, J. El Haskouri, J. Alamo, A. Beltran, D. Beltran, S. Mendioroz, M. D. Marcos, P. Amoros, *Adv. Mater.* **1999**, *11*, 379–381.
- [58] S. Valange, J. Guth, F. Kolenda, S. Lacombe, Z. Gabelica, *Microporous Mesoporous Mater.* **2000**, *35–36*, 597–607.
- [59] X. Liu, Y. Wei, D. Jin, W. Shih, *Mater. Lett.* **2000**, *42*, 143–149.
- [60] F. Schüth, *Chem. Mater.* **2001**, *13*, 3184–3195.
- [61] Z. Zhang, R. W. Hicks, T. R. Pauly, T. J. Pinnavaia, *J. Am. Chem. Soc.* **2002**, *124*, 1592–1593.
- [62] Z. Zhang, T. J. Pinnavaia, *J. Am. Chem. Soc.* **2002**, *124*, 12294–12301.
- [63] R. W. Hicks, T. J. Pinnavaia, *Chem. Mater.* **2003**, *15*, 78–82.
- [64] R. W. Hicks, Z. Zhang, T. J. Pinnavaia, Patent WO03011759 **2003**, 1–12.
- [65] *Aquatic Surface Chemistry* (Ed.: P. W. Schindler, W. Stumm), Wiley-Interscience, New York, **1987**, p. 83.
- [66] V. E. Henrich, P. A. Cox, *The Surface Science of Metal Oxides*, Cambridge Univ. Press, Cambridge, UK, **1994**.
- [67] P. P. Mardilovich, A. N. Govyadinov, N. I. Mazurenko, R. Paterson, *J. Membr. Sci.* **1995**, *98*, 143–155.
- [68] G. E. Brown, Jr., V. E. Henrich, W. H. Casey, D. L. Clark, C. Eggleston, A. Felmy, D. W. Goodman, M. Grätzel, G. Maciel, M. I. McCarthy, K. H. Nealon, D. A. Sverjensky, M. F. Toney, J. M. Zachara, *Chem. Rev.* **1999**, *99*, 77–174.
- [69] G. A. Parks, *Chem. Rev.* **1965**, *65*, 177–198.
- [70] J. P. Brunelle, *Pure Appl. Chem.* **1978**, *50*, 1211–1229.
- [71] A. Daggetti, G. Lodi, S. Trasatti, *Mater. Chem. Phys.* **1983**, *8*, 1–90.
- [72] J. Lyklema, *Fundamentals of Interface and Colloid Science*, Academic Press Inc., San Diego, **1991**.
- [73] C. P. Schulthess, D. L. Sparks, *Soil. Sci. Soc. Am. J.* **1986**, *50*, 1406–1411.

- [74] K. W. Goyne, A. R. Zimmerman, B. L. Newalkar, S. Komarneni, S. L. Brantley, J. Chorover, *J. Porous Mater.* **2002**, *9*, 243–256.
- [75] J. Ganor, J. Cama, V. Metz, *J. Colloid Interface Sci.* **2003**, *264*, 67–75.
- [76] C. R. Evanko, R. F. Delisio, D. A. Dzombak, J. W. Novak, Jr., *Colloids Surf. A: Physicochem. Eng. Aspects* **1997**, *125*, 95–107.
- [77] C. Contescu, J. Jagiello, J. A. Schwarz, *Langmuir* **1993**, *9*, 1754–1765.
- [78] K. Nagashima, F. D. Blum, *J. Colloid Interface Sci.* **1999**, *217*, 28–36.
- [79] S. Subramanian, J. S. Noh, J. A. Schwarz, *J. Catal.* **1988**, *114*, 433–439.
- [80] C. Contescu, A. Contescu, J. A. Schwarz, *J. Phys. Chem.* **1994**, *98*, 4327–4335.
- [81] T. Hiemstra, H. Yong, W. H. Van Riemsdijk, *Langmuir* **1999**, *15*, 5942–5955.
- [82] C. Contescu, V. T. Popa, J. A. Schwarz, *J. Colloid Interface Sci.* **1996**, *180*, 149–161.
- [83] J. L. Paulhiac, O. Clause, *J. Am. Chem. Soc.* **1993**, *115*, 11602–11603.
- [84] J. C. Parker, L. W. Zelazny, S. Sampath, W. G. Harris, *Soil Sci. Soc. Am. J.* **1979**, *43*, 668–674.
- [85] W. Stumm, J. J. Morgan, *Aquatic Chemistry: An Introduction Emphasizing Chemical Equilibria*, in *Natural Waters*, 2nd ed., John Wiley & Sons, Inc., New York, **1981**.
- [86] L. J. Criscenti, D. A. Sverjensky, *Am. J. Sci.* **1999**, *299*, 828–899.
- [87] K. Bourikas, T. Hiemstra, W. H. Van Riemsdijk, *Langmuir* **2001**, *17*, 749–756.
- [88] K. Shibata, T. Kiyoura, J. Kitagawa, T. Sumiyoshi, K. Tanabe, *Bull. Chem. Soc. Jpn.* **1973**, *46*, 2985–2988.
- [89] C. Contescu, V. T. Popa, J. B. Miller, E. I. Ko, J. A. Schwarz, *Chem. Eng. J.* **1996**, *64*, 265–272.
- [90] J. A. Davis, J. O. Leckie, *J. Colloid Interface Sci.* **1978**, *67*, 90–107.
- [91] L. K. Koopal, W. H. Van Riemsdijk, M. G. Roffey, *J. Colloid Interface Sci.* **1987**, *118*, 117–135.
- [92] W. Piasecki, *Phys. Chem. Chem. Phys.* **2003**, *5*, 713–719.
- [93] C. Contescu, J. A. Schwarz, *Appl. Catal. A: General* **1994**, *118*, L5–L10.
- [94] C. Contescu, V. T. Popa, J. B. Miller, E. I. Ko, J. A. Schwarz, *J. Catal.* **1995**, *157*, 244–258.
- [95] J. Jagiello, T. J. Bandoz, K. Putyera, J. A. Schwarz, *J. Colloid Interface Sci.* **1995**, *172*, 341–346.
- [96] T. J. Bandoz, J. Jagiello, J. A. Schwarz, *J. Phys. Chem.* **1995**, *99*, 13522–13527.
- [97] T. J. Bandoz, J. Jagiello, J. A. Schwarz, *J. Phys. Chem.* **1996**, *100*, 15569–15574.
- [98] T. J. Bandoz, J. Jagiello, C. Contescu, J. A. Schwarz, *Carbon* **1993**, *31*, 1193–1202.
- [99] A. M. Puziy, O. I. Poddubnaya, J. A. Ritter, A. D. Ebner, Ch. E. Holland, *Carbon* **2001**, *39*, 2313–2324.
- [100] J. C. M. de Wit, W. H. Van Riemsdijk, L. K. Koopal, *Environ. Sci. Technol.* **1993**, *27*, 2015–2022.
- [101] M. N. Nederlof, J. C. M. de Wit, W. H. Van Riemsdijk, L. K. Koopal, *Environ. Sci. Technol.* **1993**, *27*, 846–856.
- [102] G. H. Bolt, W. H. Van Riemsdijk, *Aquatic Surface Chemistry* (Ed.: W. Stumm), Wiley, New York, **1987**, p. 127–164.
- [103] J. Jagiello, *Langmuir* **1994**, *10*, 2778–2785.
- [104] F. Villieras, J. L. Michot, F. Bardot, J. M. Cases, M. François, W. Rudziński, *Langmuir* **1997**, *13*, 1104–1117.
- [105] M. Černík, M. Borkovec, J. C. Westall, *Environ. Sci. Technol.* **1995**, *29*, 413–425.
- [106] J. Bersillon, F. Villieras, F. Bardot, T. Gerner, J. Cases, *J. Colloid Interface Sci.* **2001**, *240*, 400–411.
- [107] B. Prélôt, R. Charmas, P. Zarzycki, F. Thomas, F. Villieras, W. Piasecki, W. Rudziński, *J. Phys. Chem. B* **2002**, *106*, 13280–13286.
- [108] J. Kijenski, A. Baiker, *Catal. Today* **1989**, *5*, 1–120.
- [109] P. Chu, E. E. Petersen, C. J. Radke, *J. Catal.* **1989**, *117*, 52–70.
- [110] L. Vordonis, N. Spanos, P. G. Koutsoukos, A. Lycourghiotis, *Langmuir* **1992**, *8*, 1736–1743.
- [111] J. C. Summers, S. A. Ausen, *J. Catal.* **1978**, *52*, 445–452.
- [112] K. Hadjiivanov, D. Klissurski, M. Kantcheva, A. Davydov, *J. Chem. Soc., Faraday Trans.* **1991**, *87*, 907–911.
- [113] M. Adachi, C. Contescu, J. A. Schwarz, *J. Catal.* **1996**, *158*, 411–419.
- [114] K. Bourikas, Ch. Kordulis, J. Vakros, A. Lycourghiotis, *Adv. Colloid Interface Sci.* **2004**, *110*, 97–120.
- [115] J. B. d'Espinose de la Caillerie, M. Kermarec, O. Clause, *J. Am. Chem. Soc.* **1995**, *117*, 11471–11481.

Received: April 22, 2005

Published Online: August 2, 2005